PHYSICAL REVIEW E, VOLUME 65, 061101

Stochastic resonance for motion of flexible macromolecules in solution

Igor E. Dikshtein
Institute of Radioengineering and Electronics, Russian Academy of Sciences, Mokhovaya Strasse 11, 103907 Moscow, Russia

Dmitri V. Kuznetsov
Institute of Biochemical Physics, Russian Academy of Sciences, Kosygin Strasse 4, 117977, Moscow, Russia

Lutz Schimansky-Geier
Institute fur Physik, Humboldt Universitat zu Berlin, D-10115, Berlin, Germany

(Received 29 January 2002; published 10 June 2002)

We consider a dilute or semidilute polymer solution with localized attracting centers near a flat phase boundary and assume it driven by both stochastic and periodic forces. The attracting inhomogeneities restrict the free motion of macromolecules and play the role of fixed pinning centers. The flat boundary is modeled by a bistable potential whose minima attract the movable polymer segments between neighboring pinning points. We study the motion of these segments. The stochastic forces lead to stochastic oscillations of the polymer parts between the two potential wells near the phase boundary. Application of a small temporal periodic force can synchronize these oscillations and leads to the phenomenon of stochastic resonance for a nonvanishing noise intensity. As an outcome of our theory in agreement with numerical simulations, the resonance is stronger for wider and/or less deep potentials and observed at smaller values of the noise intensity. Additionally, we discuss under what conditions doubly stochastic resonance of the macromolecular motion occurs, that is, if bistability of the potential near the boundary originates in the action of multiplicative noise.

DOI: 10.1103/PhysRevE.65.061101 PACS number(s): 05.40.Ca, 02.50.Ey, 36.20.Ey, 61.25.Hq

I. INTRODUCTION

The presence of noise in a nonlinear dynamical system is known to lead to cooperative effects, including stochastic resonance (SR) [1–3] and noise-induced phase transitions [4–6]. SR is a cooperative phenomenon, in which a response of the bistable or threshold stochastic system to a small periodic signal, as well as the signal-to-noise ratio (SNR) at the frequency of the fundamental harmonics, can be enhanced by tuning the noise intensity to an optimal nonzero value. Recently, theoretical and experimental studies have been focused on SR in spatially distributed systems, which are very interesting for practical application in physics and biology. It has been shown in [7–9] that the response (and SNR) of a single stochastic resonator can be further enhanced, if it is embedded in an ensemble of other stochastic resonators that are properly coupled. SR for the one-dimensional (1D) and two–dimensional (2D) Ising model with Glauber dynamics in an oscillating magnetic field was studied in [10,11]. Spatiotemporal SR has been observed in excitable media [12,13] and systems described by the Swift-Hohenberg equation [14]. The SR of domain-wall motion in 1D and 2D nonuniform magnetic media was studied in [15–18].

Other examples of the ordering role of noise in nonequilibrium situations through its interaction with the nonlinearity of the system are the noise-induced phenomena in spatially extended systems (see [19] for a review). They include noise-induced patterns [20] and noise-induced phase transitions [21]. Noise-sustained phenomena have been found and investigated in noise-supported traveling structures in excitable media [22], in noise-sustained convective structures [23], and at a noise-induced phase separation [24]. Recently, SR in a system with a noise-induced nonequilibrium phase transition resulting in bistable behavior of the mean field has been reported [25]. This effect was named doubly stochastic resonance to emphasize that additive noise causes a resonancelike behavior in the structure, which in turn is induced by multiplicative noise.

In the present study we intend to consider SR for the motion of macromolecules in a bistable dissipative dilute or semidilute polymer solution with localized attracting centers. The double-well potential describes the effect of a flat boundary between two phases or solvents where polymer segments are attracted by the interiors of both phases (solvents) and repelled from the boundary. The localized attracting centers model motionless (during the considered time intervals) inhomogeneities, impurities, or long-living interchain entanglements. We assume that some polymer segments can be trapped by the centers and become motionless, as well as the centers themselves. All other polymer segments keep movement freedom restricted only by the chain connectivity with the motionless segments. Thus, the polymer segments form mostly mobile bridges between the fixed pinning points. For a dilute or semidilute solution, each ‘‘bridge’’ can be considered independently from the others, i.e., we neglect ‘‘bridge-bridge’’ interactions. If in this system the potential wells are deep, then, in equilibrium [when time-dependent fields (signals) and noise are absent], the ‘‘bridges’’ are curved into the interior of one of the two phases (with the minimum total free energy of the system). With an applied noise (random forces due to internal fluctuations or external random fields), the polymer segments are able to oscillate stochastically [26] between the potential wells. It is expected, that, with a weak periodic force (external periodic field) applied to the system, SR in the motion of the macromolecules will be observed.

In the present paper, to extract the most interesting and specific features of the macromolecular nature in the stochastic resonance environment, we will restrict our consideration to the basic dynamic polymer model, which is the Rouse model [27,28]. We will discuss some limits, where the leading factors of chain movement are reduced to more-or-less well studied SR phenomena, such as single-particle SR behavior [29]. (Depending on the system parameters, one-particle SR properties can be applied to a whole polymer or every single-chain segment.)

The paper is organized in seven more sections. In Sec. II, we present our model of the polymer chain restricted by two pinning centers and driven by periodic and noisy forces in a double-well shaped potential. The basic dynamic regimes of the system are described in Sec. III. Sections IV and V are devoted to numerical and analytical studies of SR in our model. In Sec. V, we deal with both time-independent (stationary) and time-dependent variational analytical solutions. SR of the motion of a macromolecule with free ends is studied in Sec. VI. In Sec. VII, we present the analytical results for macromolecular motion driven by multiplicative and additive noise. The conditions for the existence of doubly stochastic resonance of the macromolecule motion are determined. Section VIII concludes with a discussion of the work.

II. THE MODEL

Consider the dynamics of a single linear polymer chain composed of N segments ($N\gg 1$) with a fixed distance l between the ends. The freedom of the ends is restricted by the motionless pinning points $\mathbf{x}_0$ $(x_0=0,y_0=0,z_0=0)$ and $\mathbf{x}_N(x_N=l,y_N=0,z_N=0)$. Generally speaking, the N segments between the pinning points can be a part of a longer macromolecule trapped by pinning centers. We assume a strong pinning, i.e., the pinned segments cannot move during the considered time intervals. As we mentioned in the Introduction, the pinning centers can be caused by stable inhomogeneities and impurities in the solvent, or long-term entanglements of the considered polymer chain with other macromolecules or other segments of the same chain. Apart from the pinning points, we ignore any other bulk interactions of the chain with surrounding polymers, assuming that the chain is placed in a dilute or semidilute polymer solution. We use the standard Rouse model (ideal phantom Gaussian chain in an immobile solvent) and treat the solvent as a viscous motionless medium in which links (beads) experience friction when moving.

The Lagrange function for the polymer chain is

$$L=\frac{m}{2}\sum_{n=1}^{N-1}\dot{\mathbf{x}}_n^2-U, \tag{1}$$

where the first term stands for the kinetic-energy density, $\mathbf{x}_n$ is the position of the nth bead (link) at the time moment t, $\dot{\mathbf{x}}_n\equiv\partial\mathbf{x}_n/\partial t$, and m is the link mass. The potential energy $U=U_{\mathrm{ch}}+U_b$ contains the coupling energy due to the chain connectivity U_{ch} and the potential energy U_b of the chain near the phase boundary. For the Gaussian chain

$$U_{\mathrm{ch}}=\frac{c}{2}\sum_{n=0}^{N-1}(\mathbf{x}_{n+1}-\mathbf{x}_n)^2, \tag{2}$$

where $c=3T/a^2$ with T being the temperature in energy units and a the average intersegment distance along the chain contour [27]. We will model the field U_b as a double-well shaped potential:

$$U_b=U_0\sum_{n=1}^{N-1}\left(\frac{y_n^2}{w_0^2}-1\right)^2, \tag{3}$$

where U_0 is the height of the potential barrier between the minima, y_n is the 1D position in the direction perpendicular to the flat phase boundary, and the parameter w_0 stands for the half distance between two wells.

The equation of motion corresponding to the Lagrange function (1) can be written down as

$$\frac{d}{dt}\frac{\partial L}{\partial\dot{\mathbf{x}}_n}-\frac{\partial L}{\partial\mathbf{x}_n}=-\frac{\partial Q}{\partial\dot{\mathbf{x}}_n}+F_{\mathrm{ex}}+F_N. \tag{4}$$

Here,

$$Q(\dot{\mathbf{x}}_n)=\frac{\xi}{2}\sum_{n=1}^{N-1}\dot{\mathbf{x}}_n^2 \tag{5}$$

is the dissipative function with ξ as the friction coefficient. $F_{\mathrm{ex}}=A_0\cos(\Omega t+\phi)$ is the external periodic field (signal) applied to the system in the direction perpendicular to the phase boundary with frequency Ω and random initial phase ϕ. The value ϕ is a random variable [29], uniformly distributed over the interval $[0,2\pi]$. $F_N=\sqrt{2D}\,\eta(t)$ is the random force associated with the noise and thermal fluctuations of the polymer chain. We assume that this noise is a Gaussian white noise with zero mean and a δ function as the autocorrelation function:

$$\langle\eta(t)\rangle=0,\quad\langle\eta(t)\,\eta(t+\tau)\rangle=\delta(\tau). \tag{6}$$

D scales the noise intensity. Both time-dependent periodic and random forces are considered as global (i.e., they do not depend on the segment position $\mathbf{x}_n$) and weak (they cannot destroy the Gaussian polymer connectivity and move the pinning centers). Moreover, the weakness of the periodic force means that it does not have a sufficiently large amplitude (without noise) to move the segments from an equilibrium stable configuration formed in one potential well to a state in the other well.

For the direction perpendicular to the phase boundary (y axis) the Lagrangian equation of motion (4) with the dissipative function (5) and the Lagrange density (1) leads to

$$m\frac{\partial^2 y_n}{\partial t^2}+\xi\frac{\partial y_n}{\partial t}=c(y_{n+1}-2y_n+y_{n-1})-\frac{\partial U_b}{\partial y_n}+A_0\cos(\Omega t+\phi)+\sqrt{2D}\,\eta(t). \tag{7}$$

For overdamped dynamics, the term, that arises from the kinetic-energy density can be neglected and Eq. (7) simplifies to

$$\xi\frac{\partial y_n}{\partial t}=c(y_{n+1}-2y_n+y_{n-1})-\frac{\partial U_b}{\partial y_n}+A_0\cos(\Omega t+\phi)+\sqrt{2D}\,\eta(t). \tag{8}$$

The motion of polymer segments in the directions parallel to the phase boundary (x and z axes) is not affected by the potential U_b and the external field F_{ex}. This motion is described only by the friction, chain connectivity, and random forces. We assume that this simple parallel motion does not disturb Eq. (8).

The pinning conditions impose important restrictions on the polymer motion. Assuming that the pinning centers for this chain are localized on the phase boundary (i.e., on the top of the potential barrier between two minima, $y=0$), we can write the conditions as

$$x_0=0,\quad y_0=0,\quad z_0=0$$

$$\text{and}\quad x_N=l,\quad y_N=0,\quad z_N=0. \tag{9}$$

Below, our numerical (Sec. IV) and analytical (Sec. V) studies are based on Eq. (8) with the conditions (9). Both these studies exhibit SR behavior for the polymer motion and lead to results that agree qualitatively.

III. BASIC DYNAMIC REGIMES

In Eqs. (2), (7), and (8) we have assumed a Gaussian type of interlink polymer connectivity. However, if the characteristic size of the link-link connectivity is much shorter than all other characteristic distances of the considered system, then any particular choice of the polymer model (dealing with microscopic scales) does not essentially affect the results following from Eq. (8). Thus, in the last case we can apply our results to macromolecules with any mechanism of chain flexibility.

We consider phenomenologically and compare possible regimes of polymer behavior in the model described above for two types of macromolecule: Gaussian beads and persistent (wormlike) polymers. The physical properties of linear polymers in bulk are determined by the following parameters with the dimension of length: the total length of the chain $L=Na$, the mean size (for instance, the radius of gyration) of an unperturbed macromolecule $R_0=(Na^2/6)^{1/2}$, the average distance between neighboring beads a, and the bead diameter d for the Gaussian model; and the length L, the unperturbed mean size R_0, the persistent length a, and the macromolecule width d for the persistent model. To consider long polymers with $N\gg1$ we have $a\ll R_0\ll L$. The polymer chain dynamics depends on the relations between these parameters and other system parameters with the dimension of length: the distance between pinning points l and the effective width $w\sim w_0\sqrt{T/U_0}$ of the bistable potential.

The effect of the distance l on the system properties is important for $l\sim L$ only, where the chain has to be strongly stretched along the potential wells and the polymer can be described as a stiff string. For $w<l\sim L$ the string can obey stochastic resonance, as described in our previous paper [30].

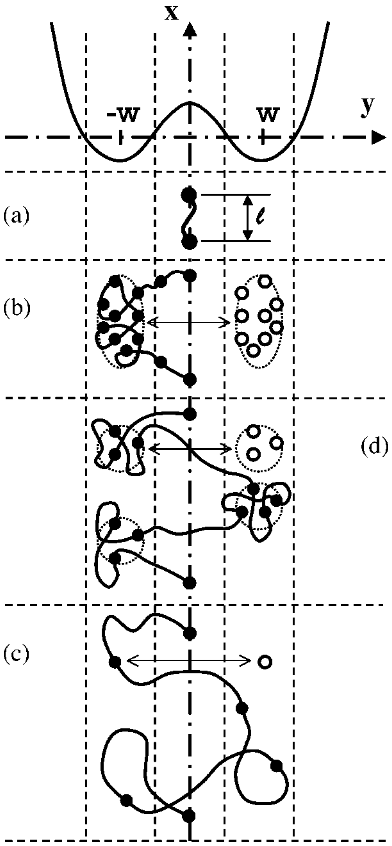

FIG. 1. Sketch of polymers following different dynamic regimes of the considered model: (a) very wide potential wells ($w>L$), (b) relatively wide potential wells ($R_0\ll w\ll L$), (c) narrow potential wells ($d\ll w\ll a$) for Gaussian chains, and (d) intermediate width wells ($a\ll w\ll R_0$).

Now we consider a different case $l\ll L$, where the effect of the potential-well width w is much more important than the effect of l. For $d\ll a\ll R_0\ll L$ and $l\ll L$ we can observe the following dynamic regimes in the system (the corresponding schematic pictures of chain configurations in these regimes are shown in Fig. 1).

(a) For very wide potential wells ($w>L$), the bistable potential does not essentially affect the polymer chain. The segments are not able to reach potential wells without extremely strong stretching and they are placed in the potential barrier area along the boundary surface [Fig. 1(a)]. SR is unreachable in this case and therefore to define any specific properties of our model we need to consider other conditions.

(b) For relatively wide potential wells ($R_0\ll w\ll L$), almost all the chain segments (the whole "bridge") have to be placed in one of the two potential wells. A state with polymer segments present in both potential wells would have a much higher free energy due to the large fraction of high-energy segments placed in the potential barrier area (to connect segments in the different wells). In the one-well state, only the segments neighboring (along the chain contour) the pinned segment are placed in the potential barrier area; this is inevitable and the fraction of such segments (with respect to the total number of chain segments) is very low. [For case (a) with $w > L$, even a one-well state would have only the neighboring segments placed in the potential barrier area, because the total chain length L would not be long enough to reach the potential wells.] Now, under random and periodic forces, the ''bridge'' can move from the first potential well to the other one mostly as a whole, because an alternative transition by parts would required a much higher activation energy. Thus, the leading dynamic properties of the considered polymer chain in the system driven by random and periodic global forces can be described as for a single solid particle under the same forces [Fig. 1(b)], that is, a system with a well-studied SR phenomenon (see, for instance, [29]). This behavior describes the macromolecule as a whole and, therefore, it does not depend on the polymer microscopic structure, i.e., on the selection of a specific polymer model.

(c) For narrow potential wells $(d \ll w \ll a)$, the system behavior strongly depends on the microscopic polymer structure. Now, for the Gaussian chain, each polymer bead can be considered as separate (disconnected from others along the chain contour). This occurs because the potential-well width w is much shorter than the interbead connectivity length a and thus the beads do not experience any restrictions arising from the connectivity even if the neighboring beads are placed in two different wells. Therefore, again as in the previous point (b), the problem is reduced to the motion of separate particles in the system driven by random and periodic forces [Fig. 1(c)]. The principal difference from the case above is that now we deal with the ''separated'' beads instead of the separate chains, moving as a single particle. However, in the present case this behavior takes place for the Gaussian beads and ceases to be valid for some other models. For instance, the persistent chain has an orientation memory along the contour distance a, which now is much longer than the potential width w. Therefore, the wormlike polymer can be described as a ''hose'' lying along a well and, in some places, rolling over the barrier between the wells. This behavior is quite different from the dynamics of separate segments. Thus, now for the wormlike polymers the connectivity effects are highly important and the problem cannot be reduced to the separate particles.

(d) The case with intermediate width w $(a \ll w \ll R_0)$ seems to be the most interesting. On the one hand, now the whole chain cannot be easily placed in one potential well only (as it was for $R_0 \ll w \ll L$). It tends to spread over both potential wells to decrease the compression energy, which is proportional to R^2/w^2. On the other hand, even for the Gaussian chain the intersegment connectivity plays a crucial role. Unlike the case of $d \ll w \ll a$, the neighboring beads cannot be placed into the different wells without a strong stretching of the interbead distance with an energy penalty proportional to w^2/a^2. Now the motion between the potential wells occurs for strongly correlated beads. This can lead to motion by neighboring chain portions (composed of a few or many neighboring segments along the chain contour).

All the basic regimes (a)–(d) are covered by Eq. (8). Indeed, for the Gaussian model, in Eqs. (2), (7), and (8) the coefficient $c = 3T/a^2$. Therefore, the first term on the right hand sides of Eqs. (7) and (8) is proportional to T/a^2. Meanwhile, the second one $\partial U_b/\partial y_n \sim U_0/w^2$. The first term can be neglected (i.e., we have the single-particle problem for each separatelike bead) if we follow the condition (c) with $w \ll a$. For the case (b), when $R \sim N^{1/2} a \ll w$ (for a long polymer with $N \gg 1$), the chain connectivity (the first term) dominates over all other contributions unless the macromolecule moves as a whole. For the intermediate case (d) all the contributions in Eq. (8) are equally important. The condition (a) with $w > L$ corresponds to the leading role of the chain connectivity.

In the next section we will analyze numerically the model equation (8) with the conditions (9) for all the regimes mentioned above.

IV. NUMERICAL TREATMENT

Due to the action of the boundary force $F_b = -\partial U_b/\partial y_n$, the polymer segments tend to move from the boundary plane $(y=0)$ to the potential wells. Random and periodic forces change the depths of the potential wells and cause ''flip-flop'' transitions of the segments between two stable symmetric states. Our main goal here is to consider the dynamics of these oscillations as a function of the noise force and the effective width of the bistable potential. The amplitude A_0 of the periodic force is assumed to be sufficiently small so that the interwell jumps of the segments would not occur without noise (i.e., the jumps are initiated by noise). However, as will be seen below, the periodic force can synchronize these jumps.

Equation (8) was simulated by a standard Euler algorithm [31] with a time step $\Delta t = 10^{-3}$ taking account of the pinning conditions (9). A noise in the Stratonovich sense was introduced into the algorithm by means of a standard procedure [32]. To ensure the reliability of the program, the convergence to a stationary analytic solution for the potential U was tested and observed. It was found that the effect of temporal global noise results approximately in a stochastic change of the polymer elongation.

In the numerical analysis, the stochastic dynamics is further reduced to two-state dynamics: $+1$ state when the average location of the polymer is above the $y=0$ plane and -1 state when it is below. The response (output) of the system with respect to the noise and periodic signal can be written as

$$q(t) = \operatorname{sgn}\left(\sum_{n=1}^{N-1} y_n \right) = \pm 1. \tag{10}$$

The binary time series, e.g.,

$$q(t) = \ldots, +1, +1, -1, +1, -1, -1, -1, +1, \ldots, \tag{11}$$

resulting from simulations of Eq. (8) over 2000 time units (corresponding to 2×10^6 time steps) were processed by a Fourier analysis that was carried out by a fast Fourier transform (FFT) algorithm. To minimize the errors arising from the FFT aliasing problem, a signal frequency Ω matching

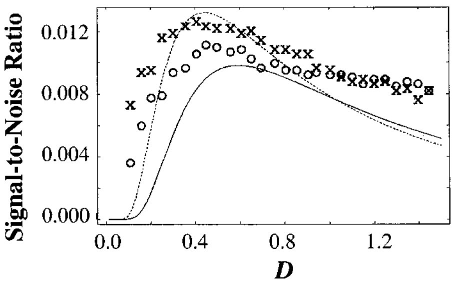

FIG. 2. Numerically determined SNR versus noise strength D for different values of the ratio w/L: 0.241 (crosses) and 0.227 (circles). The dashed and solid curves present theoretical estimations for $w/L=0.241$ and $w/L=0.227$, respectively. The other parameters are $\Omega=0.301$, $A_0=0.2$, $L=11$, $\eta_l=2$, $U_0=3$, $w_0=1$, $\Delta=5.25$, $\Delta t=10^{-3}$, and $N=15$.

one of the frequencies of the resulting discrete Fourier spectrum was chosen. The FFT used 4096 sampling points. In order to get a stationary power spectrum density (PSD), an ensemble of 50 spectra was averaged over equally distributed initial phases.

The resulting PSD, consisting of a peak at Ω and its multiples riding on a Lorentzian-like background noise, is characteristic for periodically driven stochastic overdamped nonlinear dynamics. To calculate the stochastic resonance, we studied the *signal-to-noise ratio* of the output. The ratio was defined as the weight of the first peak at Ω divided by the value of the background noise at the peak frequency. While tuning the noise intensity D, the SNR shows a clear maximum for two different values of the effective potential width (see Fig. 2). This maximum behavior is called *stochastic resonance*. Increasing the input noise intensity leads to an increased coherence between output and input signals. The reason for this behavior is a change (due to the tuning) in the stochastic time scale specifying the jumping time of the polymer.

As can be seen from Fig. 2, the SNR maximum shifts to larger values of D if the effective potential width w decreases. A way to understand this is given in the next section where we present a qualitative theoretical approach using a picture of an effective potential.

V. THEORETIC APPROACH

The continuous analog of Eq. (8) is

$$\xi \frac{\partial y(t,s)}{\partial t} = 3T \frac{\partial^2 y(t,s)}{\partial s^2} - \frac{\partial U_b(y)}{\partial y} + A_0 \cos(\Omega t+\phi) + \sqrt{2D}\,\eta(t), \qquad (12)$$

where the 1D position $y_n(t)$ of the polymer segment $n=1,\ldots,N$ at the time moment t was transformed to the position $y(t,s)$ of the point s $(0\leqslant s\leqslant L=Na)$ along the polymer contour, $y_n(t)\rightarrow y(t,na)\rightarrow y(t,s)$, and the explicit expression $c=3T/a^2$ was substituted. The pinning conditions (9) for the 1D position $y(t,s)$ in the continuous limit can be written as

$$y(s=0)=0, \quad y(s=L)=0, \qquad (13)$$

where $L=Na$ is the total length of the chain between pinning points.

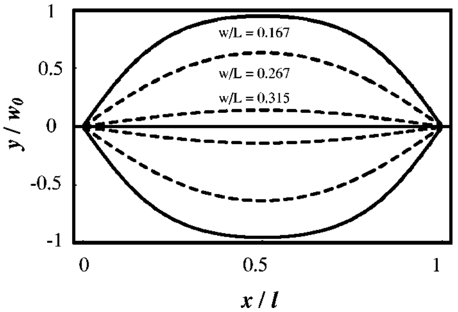

FIG. 3. Stationary configurations of a macromolecule for $M=1$ and the following values of the w/L ratio: 0.167, 0.267, and 0.315.

A. Stationary solution

If $F_{ex}=0$ and $F_N=0$ (i.e., $A_0=0$ and $D=0$), Eq. (12) with the pinning conditions (13) possesses the following stationary (time independent) solutions: (i) the trivial solution

$$y(s)=0, \qquad (14)$$

corresponding to a polymer chain with segments placed on the phase boundary, and (ii) solutions of the type

$$y(s)=\pm b_m \,\mathrm{sn}(qs,k), \qquad (15)$$

corresponding to the macromolecule curved inside the phases. Here sn is the Jacobian elliptic sine [33], $b_m=w_0\sqrt{2(1-q^2w^2)}$, $k=\sqrt{(qw)^{-2}-1}$, $w=(w_0/2)\sqrt{3T/U_0}$, and q is the integration constant.

Using the conditions (13), the equation for calculation of the integration constant q takes the form

$$q=\frac{2M}{L}K(k), \qquad (16)$$

where $K(k)$ is the complete elliptic integral of the first kind [33], $M=1,2,\ldots$.

Stationary polymer configurations for different values of the ratio w/L are shown in Fig. 3. This ratio $w/L \sim (w_0/L)\sqrt{T/U_0}$ is a measure of the constraints experienced by a polymer chain of length L due to the bistable boundary potential U_b: the stronger the constraints (smaller width w_0 and higher barrier U_0), the lower is the value w/L.

For wide and/or shallow potentials with $w/L\geqslant 1/\pi$, the boundary force caused by the bistable potential is not sufficient to disturb the polymer from the conformation corresponding to the solution $y(s)\equiv 0$, which would occur without any boundary fields (i.e., at $U_0=0$) or for extremely wide potential wells ($w_0\rightarrow\infty$). As we mentioned in Sec. III, in this case (where the bistable potential does not affect the polymer) the SR is unreachable. However, as shown in Sec. VII, bimodality of the macromolecule configuration can be induced by multiplicative noise. Therefore, SR of the macromolecule motion can exist if the system is simultaneously driven by multiplicative and additive noise.

For lower values $w/L \leqslant 1/\pi$, the solution (15) describes states with a lower energy than for Eq. (14). For $M>1$ the corresponding dependency $y(s)$ can have more than one extremum between $s=0$ and $s=L$ at $s=mL/(2M)(m=1,\ldots,M)$. However, for $w/L \leqslant 1/\pi$ the chain configuration with $M=1$ has the minimal energy.

The stationary nonzero solution (15) can be substantially simplified in the limiting cases of very low and very high w/L ratios. For $L \gg w$ and $M=1$, we have

$$y(s)=\begin{cases} \pm B\tanh[s/(\sqrt{2}w)] & \text{for } 0<s<L/2, \\ \pm B\tanh[(L-s)/(\sqrt{2}w)] & \text{for } L/2<s<L, \end{cases} \tag{17}$$

with

$$B=w_0\left[1-4\exp\left(-\frac{L}{\sqrt{2}w}\right)\right] \tag{18}$$

and the other parameters given by

$$k=1-8\exp\left(-\frac{L}{\sqrt{2}w}\right), \tag{19}$$

$$q=\sqrt{2}w\left[1+4\exp\left(-\frac{L}{\sqrt{2}w}\right)\right]. \tag{20}$$

For $L \cong \pi M w (M=1,2,\ldots)$, one gets

$$y(s)=\pm B\sin(qs), \tag{21}$$

where

$$B=\sqrt{\frac{8}{3}}\delta w_0\left(1-\frac{25}{24}\delta^2\right), \quad k=\sqrt{\frac{4}{3}}\delta\left(1-\frac{3}{8}\delta^2\right), \tag{22}$$

$$q=\frac{\pi}{L}\left(1+\frac{1}{3}\delta^2\right), \quad \delta=\sqrt{\frac{L}{\pi M w}-1}. \tag{23}$$

From the equations above, it follows that the macromolecule becomes curved inside the phases for $L \geqslant \pi w$. For $\pi w \leqslant L \leqslant 2\pi w$ the macromolecule has two stable symmetric configurations. For $\pi M w \leqslant L \leqslant \pi(M+1)w$ the macromolecule has two stable and $2(M-1)$ metastable configurations. It follows from Eqs. (15), (17), and (21) that the chain configuration depends on the ratio w/L of the effective potential width w to the total chain length L: the larger T and the smaller L and the potential gradient $\sqrt{U_0}/w_0$, the less macromolecule dangles into the phase interiors.

B. Variational solution

According to El'sgoltz [34], the approximate variational solution of our problem should be sought in the form of a finite combination of trial functions with unknown coefficients depending on time. This approximation is more adequate for our case than other methods, for example, the Ritz method. As a first approximation, the ansatz

$$y(s)=b(t)\,\mathrm{sn}(qs,k) \tag{24}$$

was used. The motivation to search for the solution in the form above is given by the stationary solution of the problem, which is the factor in Eq. (24). The amplitude $b(t)$ represents an elongation. For the stationary case it is equal to $\pm b_m$. The results of our numerical simulation also suggest the usage of this ansatz. The benefit of applying this ansatz is that our 2D problem is reduced to a 1D one.

Substituting the ansatz (24) into the energy (1) and dissipative function Q (5), and integrating them over s, we get the functionals $U[b(t)]$ and $Q[b(t)]$. Furthermore, we will consider only small deviations of the macromolecule from the $y=0$ plane, that is, small elongations $b(t)$. After carrying out the integration over s, we obtain expansions of $U[b(t)]$ and $Q[b(t)]$ as power series in $b(t)$ up to fourth order:

$$U[b(t)]=U_{\mathrm{eff}}\left(\frac{b^2}{b_m^2}-1\right)^2, \tag{25}$$

$$Q[b(t)]=\frac{1}{2}\xi\Lambda\left(\frac{\partial b}{\partial t}\right)^2, \tag{26}$$

where

$$U_{\mathrm{eff}}=\frac{4}{3}\frac{U_0L}{1+k^2}\left[\frac{2+k^2}{1+k^2}-\frac{4}{qL}E(k)\right],$$

$$b_m=w_0\sqrt{\frac{2k^2}{1+k^2}}, \quad \Lambda=\frac{L}{k^2}\left[1-\frac{2}{qL}E(k)\right], \tag{27}$$

with $E(k)$ being the complete elliptic function of the second kind [33].

In the overdamped limit the reduced equation of motion for the dynamics of the elongation

$$\frac{\delta Q(\partial b/\partial t)}{\delta(\partial b/\partial t)}=-\frac{\delta U[b]}{\delta b}+A_{0\mathrm{eff}}\cos(\Omega t+\phi) + \sqrt{2D_{\mathrm{eff}}}\xi(t) \tag{28}$$

takes the form

$$\xi\frac{\partial b(t)}{\partial t}=\frac{4U_{0r}}{b_m}\left(\frac{b(t)}{b_m}-\frac{b^3(t)}{b_m^3}\right)+A_{0r}\cos(\Omega t+\phi) + \sqrt{2D_r}\xi(t) \tag{29}$$

with

$$A_{0\mathrm{eff}}=\frac{A_0}{qk}\ln\frac{1+k}{1-k}, \quad D_{\mathrm{eff}}=\frac{D}{q^2k^2}\ln^2\frac{1+k}{1-k}, \tag{30}$$

and

$$U_{0r}=\frac{U_{\mathrm{eff}}}{\Lambda},\quad A_{0r}=\frac{A_{0\mathrm{eff}}}{\Lambda},\quad D_r=\frac{D_{\mathrm{eff}}}{\Lambda^2}. \tag{31}$$

Equation (29) describes nothing but the stochastic motion of a Brownian particle driven by a periodic signal with the rescaled signal amplitude A_{0r} and a noise with rescaled intensity D_r. The particle is placed in a double-well potential with the distance between two wells b_m and the potential barrier height between wells U_{0r}. This is one of the best studied systems in the theory of SR and we are able to apply the earlier results by rescaling the parameters according to our problem. In particular, we use the McNamara and Wiesenfeld theory [29], where the dynamics is further reduced to a periodically driven two-state random walk in the limit of small amplitudes. This theory, like the linear response theory for the dynamics between two wells [2], is in sufficiently good agreement with the numerical treatment in Sec. IV.

Two discrete states of elongations $b(t)=\pm b_m$ will be considered below. Denoting the probabilities of finding the macromolecule in the right and left wells of the bistable potential (stable states) at time t by $n_+(t)$ and $n_-(t)$, respectively, the master equation reads

$$\frac{dn_\pm}{dt}=-[W_+(t)+W_-(t)]n_\pm+W_\mp(t), \tag{32}$$

where $W_+(t)$ and $W_-(t)$ are the transition probability densities corresponding to the jumps $(+)\rightarrow(-)$ and $(+)\leftarrow(-)$, respectively, $n_-(t)=1-n_+(t)$. Following [29], the modified Kramers rate can be used for the transition probability densities:

$$W_\pm(t)=r_K\exp\left[\pm\frac{\xi b_m A_{0r}}{D_r}\cos(\Omega t+\phi)\right], \tag{33}$$

with $r_K=(2\sqrt{2}/\pi)[U_{0r}/(\xi b_m^2)]\exp(-\xi U_{0r}/D_r)$ being the Kramers rate for $A_0=0$ (see [35]). The expression (33) holds true only in the adiabatic approach, where the signal is sufficiently slow in comparison with all relevant time scales of the system. This means that the temporal change of the adiabatic potential (25) has to be slow in comparison with the intrawell relaxation.

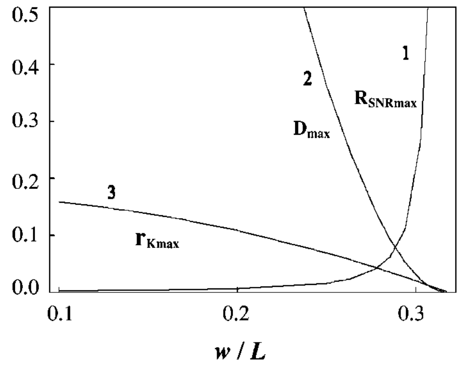

FIG. 4. The analytical dependence of $\mathrm{R}_{\mathrm{SNR}_{\max}}$ (curve 1), $D_{\max}$ (curve 2), and $r_{K\max}$ (curve 3) versus w/L. For parameters, see caption to Fig. 2.

Using the Kramers rate for the stochastic process (33), the two-state theory [29] can be directly applied. Since in the limit of small amplitudes $[A_{0r}\ll D_r/(\xi b_m)]$ the power arising from the signal is much smaller than the power of the whole spectrum, the two-state output can be easily calculated. To make the analysis independent of the initial state and, hence, to transform the problem into a stationary process, the resulting expressions were averaged over a random initial phase (assuming that it is equally distributed) of the periodic output. The resulting power spectrum of the two-state theory,

$$\begin{aligned}S(\omega)&=\frac{1}{2\pi}\int_0^{2\pi}S(\omega,\theta)d\theta\\&=S_N(\omega)+\frac{\pi}{2}\left(\frac{\xi b_m A_{0r}}{D_r}\right)^2\frac{4r_K^2 b_m^2}{4r_K^2+\omega^2}\\&\quad\times[\delta(\omega-\Omega)+\delta(\omega+\Omega)],\end{aligned} \tag{34}$$

consists of weighted δ functions, due to the periodic driving, and a continuous Lorentzian-like noise background [29,2]

$$S_N(\omega)=\left[1-\frac{1}{2}\left(\frac{\xi b_m A_{0r}}{D_r}\right)^2\frac{4r_K^2}{4r_K^2+\Omega^2}\right]\frac{4r_K b_m^2}{4r_K^2+\omega^2}. \tag{35}$$

Therefore, within the described limitations, the SNR (the ratio of the weight of the δ function and the noise background at Ω) can be written as

$$R_{\mathrm{SNR}}\approx\sqrt{2}\,\frac{\xi U_{0r}A_{0r}^2}{\Delta D_r^2}\exp\left(-\frac{\xi U_{0r}}{D_r}\right), \tag{36}$$

with Δ being the width of a frequency bin in Hz (see [36]). The above analytical dependencies of the SNR on the noise intensity D are presented in Fig. 4 for different values of w/L. They exhibit the well-known bell-shaped curves. They agree qualitatively with the SNR of the numerical treatment and have maxima with the values

$$R_{\mathrm{SNR}_{\max}}=\frac{4\sqrt{2}}{e^2}\,\frac{A_0^2}{D_{\max}\Delta} \tag{37}$$

located at

$$\begin{aligned}D=D_{\max}&=\frac{8}{3}\,\frac{\xi U_0}{1+k^2}\,\frac{K(k)-E(k)}{[\ln(1+k)-\ln(1-k)]^2}\\&\quad\times\left[\frac{2+k^2}{1+k^2}K(k)-2E(k)\right].\end{aligned} \tag{38}$$

Strictly speaking, SR is not a resonance in the sense of increased response when a driving frequency is tuned to an intrinsic frequency of the system. However, there is a useful analogy with resonance since the SNR (the "response") is maximized when an input signal is tuned near a certain value $D_{\max}$.

It follows from Fig. 4 that the SNR maximum increases and shifts to a lower value of D with the growth of w/L, qualitatively as in our numerical analysis. Let us consider now the dependence of the SNR on the ratio w/L in more detail. Since the coefficients U_{eff} and $A_{0\mathrm{eff}}$ contain the parameter $1/(qL) \propto w/L$, the effective potential (25) will change on varying these parameters. As the parameter w/L increases, the effective potential (25) is smoothed, the macromolecule contracts toward the $y=0$ plane, and less noise is needed to bring the macromolecule to the other side of the potential barrier. That explains the growth of the SNR maximum and its shift to lower values of D with increasing w/L. With the estimations (18)–(20) and (23) given above, we can evaluate the corresponding limiting values of the SNR. It follows from Eqs. (37) and (38) that in the long-chain limit ($L \rightarrow \pi w$) the maximal value of the SNR and the corresponding noise intensity behave as $R_{\mathrm{SNR}_{\max}} \propto [A_0^2/(\Delta \xi U_0)] k^{-4} \propto [A_0^2/(\Delta \xi U_0)][L/(\pi w) - 1]^{-2}$ and $D_{\max} \propto \xi U_0 k^4 \propto \xi U_0 [L/(\pi w) - 1]^2$. For relatively short macromolecules ($w/L \rightarrow 0$), $R_{\mathrm{SNR}_{\max}}$ and $D_{\max}$ approach constants; in particular, we have found $R_{\mathrm{SNR}_{\max}} = 4\sqrt{2} A_0^2/(e^2 \Delta \xi U_0)$, $D_{\max} = \xi U_0/2$. The results of calculations of $R_{\mathrm{SNR}_{\max}}$ (curve 1) and $D_{\max}$ (curve 2) versus the ratio w/L are depicted in Fig. 4.

In Fig. 4 is also shown the behavior of the Kramers rate $r_{K\,\max} \equiv r_K(D=D_{\max}) = \sqrt{8} U_{0r}/(\pi e^2 \xi b_m^2)$ versus w/L (curve 3). In the limit $L \rightarrow \pi w$, the maximal rate $r_{K\,\max}$ tends to zero ($r_K \propto [U_0/(\xi w_0^2)] k^2$). For $w/L \rightarrow 0$, the rate approaches a constant $[r_K = \sqrt{8} U_0/(\pi e^2 \xi w_0^2)]$.

VI. STOCHASTIC RESONANCE OF MOTION OF A MACROMOLECULE WITH FREE ENDS

Next, the dynamics of a single macromolecule with free ends located in the double-well shaped potential (3) is studied. In this case the stationary solutions of Eq. (12) satisfying the conditions

$$\frac{\partial y}{\partial s} = 0 \tag{39}$$

at the free ends $s=0$ and $s=L$ can be written as

$$y(s) = \pm w_0 \tag{40}$$

and

$$y(s) = \pm b_m \operatorname{sn}[qs + K(k), k] \tag{41}$$

with $q = (2M/L) K(k)$ being the integration constant.

The solution (40) has the minimal energy. Therefore, the dynamics of only a chain completely located in one of the potential wells has to be further considered in this section. Thus, the equations for the power spectrum, R_{SNR}, $R_{\mathrm{SNR}_{\max}}$, and $D_{\max}$ of the two-state theory have the same forms as shown in Eqs. (34)–(38), respectively, with the replacement of b_m by w_0. The index r for U_0, A_0, and D in Eqs. (34)–(38) must be omitted. From Eqs. (34)–(38), it follows that for a macromolecule with free ends the magnitudes of R_{SNR}, $R_{\mathrm{SNR}_{\max}}$, and $D_{\max}$ do not depend on the ratio w/L.

VII. DOUBLY STOCHASTIC RESONANCE OF THE MACROMOLECULE MOTION

Finally, in this section the doubly SR of the macromolecule motion driven by multiplicative and additive noise and the periodic signal will be studied. The following set of Langevin equations describes the system considered:

$$\xi \frac{\partial y_n}{\partial t} = c(y_{n+1} - 2y_n + y_{n-1}) - \frac{\partial U_b}{\partial y_n} + \sqrt{2D_\zeta}\, \zeta_n(t) y_n + A_0 \cos(\Omega t + \phi) + \sqrt{2D}\, \eta(t). \tag{42}$$

The noisy terms $\zeta(t) y_n$ and $\eta(t)$ represent mutually uncorrelated Gaussian noise, with zero mean and correlations given by

$$\langle \zeta_n(t) \zeta_m(t+\tau) \rangle = \delta_{n,m} \delta(\tau) \tag{43}$$

and Eq. (6).

Next we consider the case of a wide and/or shallow potential with $w/L \geqslant 1/\pi$. In this case the boundary force caused by the bistable potential is not sufficient to disturb the polymer with pinned ends from the conformation corresponding to the solution $y(s) \equiv 0$ for $\zeta_n(t) = 0$. Therefore, the change in bimodality of the macromolecule configuration induced by the multiplicative noise will be our initial concern. If A_0, D, and c vanish, the time evolution of the first moment of a single segment is given simply by the drift part in the corresponding Fokker-Planck equation (Stratonovich case):

$$\xi \frac{\partial \langle y \rangle}{\partial t} = -\frac{\partial U_b(\langle y \rangle)}{\partial \langle y \rangle} + D_\zeta \langle y \rangle. \tag{44}$$

As was argued in [37], the mechanism of the noise-induced phase transitions in coupled systems can be explained by means of a short-time-evolution approximation. This means that we start with an initial Dirac δ function and follow it only for a short time, such that fluctuations are small and the probability density is well approximated by Gaussian. Suppression of fluctuations performed by coupling along the polymer chain makes this approximation appropriate in our case [38]. The equation for the maximum of the probability, which is also the average value in the approximation $\tilde{y} = \langle y \rangle$, takes the following form:

$$\xi \frac{\partial \tilde{y}}{\partial t} = -\frac{\partial U_b(\tilde{y})}{\partial \tilde{y}} + D_\zeta \tilde{y}, \tag{45}$$

which is valid if $U_b(\langle y\rangle) \gg \langle \delta y^2\rangle U_b''(\langle y\rangle)$. For this dynamics an effective potential $U_b^{\mathrm{eff}}(y)$ can be derived, which has the form

$$U_b^{\mathrm{eff}}(y) = U_b(y) + U_b^{\mathrm{noise}}(y) = U_b(y) - \frac{D_\zeta}{2} y^2$$
$$\equiv -\Delta U_b + \tilde{U}_0 \left(\frac{y^2}{\tilde{w}_0^2} - 1 \right)^2, \tag{46}$$

where

$$\Delta U_b = \frac{D_\zeta w_0^2}{2} \left(1 + \frac{D_\zeta w_0^2}{8U_0} \right),$$

$$\tilde{U}_0 = U_0 \left(1 + \frac{D_\zeta w_0^2}{4U_0} \right)^2, \quad \tilde{w}_0 = w_0 \sqrt{1 + \frac{D_\zeta w_0^2}{4U_0}}, \tag{47}$$

with $\tilde{U}_0$ and $\tilde{w}_0$ being the height of the potential barrier between the minima and the half distance between two wells renormalized by multiplicative noise. It follows from Eq. (47) that the magnitudes of $\tilde{U}_0$ and $\tilde{w}_0$ grow with an increase in the multiplicative noise intensity D_ζ.

The stationary macromolecule configurations $y(s)$ have the same forms as shown in Eqs. (14) and (15), respectively, with the replacement of U_0 and w_0 by $\tilde{U}_0$ and $\tilde{w}_0$. In this case, the ratio $w/L = [\tilde{w}_0/(2L)]\sqrt{T/\tilde{U}_0} \equiv [w_0/(2L)][1 + (D_\zeta w_0^2)/(4U_0)]^{-1/2}$, which is a measure of the polymer chain stiffness, decreases with increasing multiplicative noise intensity D_ζ. For $w/L \leqslant 1/\pi$, the pinned macromolecule driven by a multiplicative noise becomes curved.

Now, if a global external periodic force and additive noise are additionally applied to the system conventional SR can be observed. Then the equations for the power spectrum, R_{SNR}, $R_{\mathrm{SNR}_{\mathrm{max}}}$, and D_{max} of the two-state theory are described by Eqs. (34)–(38), respectively, with the replacement of U_0 and w_0 by $\tilde{U}_0$ and $\tilde{w}_0$. A decrease in the effective stiffness of the pinned polymer chain w/L with the growth of multiplicative noise intensity D_ζ leads to a decrease of the SNR maximum and its shift to higher values of D.

In conclusion, in this section we report the twofold effect of noise on the polymer dynamics. An additive noise and periodic signal causes SR of the macromolecule motion in the potential, which in its turn is induced by multiplicative noise. Following [25], this effect could be classed as doubly SR of the macromolecule motion.

VIII. CONCLUSIONS

We have demonstrated that noise can enhance the periodic component in the stochastic motion of a macromolecule. This study generalizes our previous results [30] for stochastic motion of stretched strings up to looped polymer chains. We studied SR for the motion of macromolecules in a bistable dissipative dilute or semidilute polymer solution with localized attracting centers. The double-well potential describes the effect of a flat boundary between two phases or solvents where polymer segments are attracted by the interiors of both phases (solvents) and repelled from the boundary. The localized attracting centers model motionless (during the considered time intervals) inhomogeneities, impurities, or long-living interchain entanglements. Some polymer segments can be trapped by the centers and become motionless as well as the centers themselves. All other polymer segments keep a freedom movement restricted only by the chain connectivity with the motionless segments. If in this system the potential wells are deep, then in equilibrium [when time-dependent fields (signals) and noise are absent] the polymer chains are curved into the interior of one of the two phases (with minimum total free energy of the system). With an applied additive noise (random forces due to internal fluctuations or external random fields), the polymer segments are able to oscillate stochastically [26] between the potential wells. With a weak periodic force (external periodic field) additionally applied to the system, the SNR of the output versus input noise intensity shows a maximum, which is called stochastic resonance. The SNR maximum ($R_{\mathrm{SNR}_{\mathrm{max}}}$) and its position ($D_{\mathrm{max}}$) depend significantly on the parameter w/L, which is a measure of the constraints experienced by a polymer chain of the length L due to the bistable potential. The position of the maximum shifts toward smaller noise values if the ratio w/L increases. This is due to the fact that the barrier of the effective bistable potential (25) gets smaller. Our polymer system represents an example of *array-enhanced SR*. This case of array-enhanced SR has a shift of the optimal noise to small values of its intensity with respect to the one discussed in [9]. If a multiplicative noise is applied additionally to the system the effective stiffness of the macromolecule decreases and $R_{\mathrm{SNR}_{\mathrm{max}}}$ shifts towards larger additive noise values. For a stiff macromolecule ($w/L \geqslant 1/\pi$), we demonstrate the existence of doubly SR of the macromolecule motion, which results from twofold influence of noise. It is a combined effect that consists of noise-induced bimodality of macromolecule conformations and conventional SR.

The motion of flexible macromolecules in solution is a special case of the motion of a 1D system subject to deterministic and noisy forces in bistable, dissipative media of higher dimension. Therefore, the results above are relevant for the understanding of the SR of dislocation motion in solids [39], domain and domain-wall dynamics in thin magnetic and ferroelastic films [40], and the motion of a front (a wave of transition between two states dividing two phases by a narrow moving interface) in reaction-diffusion systems [41].

ACKNOWLEDGMENT

This work was supported in part by the Russian Foundation for Basic Research (Grant No. 99-02-17404).

[1] R. Benzi, A. Sutera, and A. Vulpani, J. Phys. A **14**, 453 (1981); R. Benzi, G. Parisi, A. Sutera, and A. Vulpani, Tellus **34**, 10 (1982).

[2] L. Gammaitoni, P. Hänggi, P. Jung, and F. Marchesoni, Rev. Mod. Phys. **70**, 223 (1998); V. S. Anishchenko, A. B. Neiman, F. Moss, and L. Schimansky-Geier, Phys. Usp. **169**, 7 (1999).

[3] See http://www.pg.infnit/SR/index.html

[4] J. Smythe, F. Moss, and P. V. E. McClintock, Phys. Rev. Lett. **51**, 1062 (1983).

[5] W. Horsthemke and R. Lefever, *Noise-Induced Transitions* (Springer, Berlin, 1984).

[6] *Noise in Nonlinear Dynamical Systems*, edited by F. Moss and P. V. E. McClintock (Cambridge University Press, Cambridge, England, 1989).

[7] P. Jung, U. Behn, E. Pantazelou, and F. Moss, Phys. Rev. A **46**, R1709 (1992).

[8] J. F. Lindner, B. K. Meadows, W. L. Ditto, M. E. Inchiosa, and A. R. Bulsara, Phys. Rev. Lett. **75**, 3 (1995); Phys. Rev. E **53**, 2081 (1996).

[9] F. Marchesoni, L. Gammaitoni, and A. R. Bulsara, Phys. Rev. Lett. **76**, 2609 (1996).

[10] Z. Neda, Phys. Rev. E **51**, 5315 (1996); Phys. Lett. A **210**, 125 (1996); J. Brey and A. Prados, *ibid.* **216**, 250 (1996).

[11] U. Siewert and L. Schimansky-Geier, in *Lectures an Stochastic Dynamics*, edited by L. Schimansky-Geier and T. Pöschel, Lecture Notes in Physics (Springer, Berlin, 1997).

[12] P. Jung and G. Mayer-Kress, Phys. Rev. Lett. **74**, 2130 (1995).

[13] S. Kadar, J. Wang, and K. Showalter, Nature (London) **391**, 770 (1998).

[14] J. M. G. Vilar and J. M. Rubi, Phys. Rev. Lett. **78**, 2886 (1997).

[15] I. Dikshtein and A. Neiman, Bull. Am. Phys. Soc. **42**, 338 (1997).

[16] A. N. Grigorenko, P. I. Nikitin, and G. V. Roshchepkin, JETP **112**, 628 (1997).

[17] I. Dikshtein, A. Neiman, and L. Schimansky-Geier, Phys. Lett. A **246**, 259 (1998); J. Magn. Magn. Mater. **188**, 301 (1998).

[18] P. Ruszcynski, L. Schimansky-Geier, and I. Dikshtein, Eur. Phys. J. B **14**, 569 (2000).

[19] J. Garcia-Ojalvo and J. M. Sancho, *Noise in Spatially Extended Systems* (Springer, New York, 1999).

[20] J. Garcia-Ojalvo, A. Hernandez-Machado, and J. M. Sancho, Phys. Rev. Lett. **71**, 1542 (1993); J. M. R. Parrando, C. Van den Broek, J. Buceta, and F. J. de la Rubia, Physica A **224**, 153 (1996); A. A. Zaikin and L. Schimansky-Geier, Phys. Rev. E **58**, 4355 (1998).

[21] C. Van den Broeck, J. M. R. Parrondo, and R. Toral, Phys. Rev. Lett. **73**, 3395 (1994); C. Van den Broeck, J. M. R. Parrondo, R. Toral, and R. Kawai, Phys. Rev. E **55**, 4084 (1997).

[22] P. Jung, A. Cornell-Bell, F. Moss, S. Kadar, J. Wang, and K. Showalter, Chaos **8**, 567 (1998); P. Jung, A. Cornell-Bell, K. Madden, and F. Moss, J. Neurophysiol. **79**, 1098 (1998); J. Wang, S. Kadar, P. Jung, and K. Showalter, Phys. Rev. Lett. **82**, 855 (1999).

[23] M. Santagiustina, P. Colet, M. San Miguel, and D. Walgraef, Phys. Rev. Lett. **79**, 3633 (1997); Phys. Rev. E **58**, 3843 (1998).

[24] M. Ibanes, J. Garcia-Ojalvo, R. Toral, and J. M. Sancho, Phys. Rev. E **60**, 3597 (1999).

[25] A. A. Zaikin, J. Kurths, and L. Schimansky-Geier, Phys. Rev. Lett. **85**, 227 (2000).

[26] H. C. Ottinger, *Stochastic Processes in Polymeric Fluids* (Springer, Berlin, 1996).

[27] A. Yu. Grosberg and A. R. Khokhlov, *Statistical Physics of Macromolecules* (AIP, New York, 1994).

[28] M. Doi and S. F. Edwards, *The Theory of Polymer Dynamics* (Clarendon Press, Oxford, 1986).

[29] B. McNamara and K. Wiesenfeld, Phys. Rev. A **39**, 4854 (1989).

[30] I. E. Dikshtein, N. I. Polzikova, D. V. Kuznetsov, and L. Schimansky-Geier, J. Appl. Phys. **90**, 5425 (2001).

[31] W. H. Press, B. P. Flannery, S. A. Teukolsky, and W. T. Vetterling, *Numerical Recipes* (Cambridge University Press, New York, 1986).

[32] R. Mannella and V. Palleschi, Phys. Rev. A **40**, 3381 (1989); P. R. Drummond and I. K. Mortimer, J. Comput. Phys. **93**, 144 (1991).

[33] *Handbook of Mathematical Functions*, edited by M. Abramowitz and I. A. Stegun (Dover, New York, 1972).

[34] L. E. El'sgoltz, *Differential Equations and Variational Calculus* (Nauka, Moscow, 1969) (in Russian).

[35] P. Hänggi, P. Talkner, and M. Bokovec, Rev. Mod. Phys. **62**, 251 (1990).

[36] A. B. Hibbs, A. L. Singsaas, E. W. Jacobs, A. R. Bulsara, J. J. Bekkedahl, and F. Moss, J. Appl. Phys. **77**, 2582 (1995).

[37] C. Van den Broeck, J. M. R. Parrondo, R. Toral, and R. Kawai, Phys. Rev. E **55**, 4084 (1997).

[38] C. Van den Broeck, in *Stochastic Dynamics*, edited by L. Schimansky-Geier and T. Pöschel (Springer, Heidelberg, 1997), p. 7.

[39] J. Friedel, *Dislocations* (Addison-Wesley, Reading, MA, 1964).

[40] A. P. Malozemoff and J. C. Slonczewski, *Magnetic Domain Walls in Bubble Materials* (Academic Press, New York, 1979).

[41] A. S. Mikhailov, L. Schimansky-Geier, and W. Ebeling, Phys. Lett. **96A**, 453 (1983).